Acute Anti-allodynic Action of Gabapentin in Dorsal Horn and Primary Somatosensory Cortex: Correlation of Behavioural and Physiological Data.

SASCHA R.A. ALLES[1], MISCHA V. BANDET, KATE EPPLER, MYUNG-CHUL NOH, IAN R. WINSHIP, GLEN BAKER, KLAUS BALLANYI AND PETER A. SMITH.

Neuroscience and Mental Health Institute (SRAS, MVB, IRW, GB, KB, PAS), Departments of Psychiatry (IRW, GB), Physiology (KB) and Pharmacology (PAS, M-CN, KE) University of Alberta, Edmonton, AB, Canada T6G 2H7.

Running Title:- Cortical and Spinal Actions of Gabapentin

Corresponding Author:-
Peter A Smith, PhD
Department of Pharmacology and Neuroscience and Mental Health Institute
9.75 Medical Sciences Building, University of Alberta, Edmonton, AB T6G 2H7, CANADA
Phone + 1 780 492 2643 FAX + 1 780 492 4325 E-mail pas3@ualberta.ca

Manuscript Properties:-
43 Text Pages, 1 Table, 6 Figures (Figs 1 and 6 in colour) Abstract 250 Words,

Abbreviations:-
cHL Contralateral hind limb, CCI Chronic Constriction Injury, DRG Dorsal Root Ganglion, GBP Gabapentin, IEI Inter-event Interval, IOS Intrinsic Optical Signal, PWT Paw Withdrawal Threshold, S1 Primary Somatosensory Cortex

[1]*Present Address* Djavad Mowafaghian Centre for Brain Health and Michael Smith Laboratories, University of British Columbia, #4541 - 2215 Wesbrook Mall, Vancouver BC, V6T 1Z3

ABSTRACT

Neuropathic pain is a debilitating consequence of neuronal injury or disease. Although first line treatments include the alpha-2-delta (α2δ)-ligands, pregabalin and gabapentin (GBP), the mechanism of their anti-allodynic action is poorly understood. One specific paradox is that GBP relieves signs of neuropathic pain in animal models within 30min of an intraperitoneal (IP) injection yet its actions *in vitro* on spinal dorsal horn or primary afferent neurons take hours to develop. We found, using confocal Ca^{2+} imaging, that *substantia gelatinosa* neurons obtained *ex vivo* from rats subjected to sciatic chronic constriction injury (CCI) were more excitable than controls. We confirmed that GBP (100mg/kg) attenuated mechanical allodynia in animals subject to CCI within 30min of IP injection. S*ubstantia gelatinosa* neurons obtained *ex vivo* from these animals no longer displayed CCI-induced increased excitability.

Electrophysiological analysis of *substantia gelatinosa* neurons *ex vivo* suggest that rapidly developing *in vivo* anti-allodynic effects of GBP i) are mediated intracellularly, ii) involve actions on the neurotransmitter release machinery and iii) depend on decreased excitatory synaptic drive to excitatory neurons without major actions on inhibitory neurons or on intrinsic neuronal excitability. Experiments using *in vivo* Ca^{2+} imaging showed that 100mg/kg GBP also suppressed the response of the S1 somatosensory cortex of CCI rats, but not that of control rats, to vibrotactile stimulation.

Since the level of α2δ1 protein is increased in primary afferent fibres after sciatic CCI, we suggest this dictates the rate of GBP action; rapidly developing actions can only be seen when α2δ1 levels are elevated.

KEYWORDS

Neuropathic Pain; Electrophysiology: *In vivo* calcium imaging; Alpha 2 delta; *Substantia gelatinosa*; Synaptic transmission.

HIGHLIGHTS

- Gabapentin (GBP) relieves neuropathic pain in animal models within 30min
- Spinal cord slices obtained *ex vivo* from GBP-treated rats have reduced excitability
- Synaptic drive to excitatory *substantia gelatinosa* neurons is decreased
- GBP actions *in vivo* are mediated intracellularly
- GBP affects the neurotransmitter release machinery *in vivo*

1. Introduction

Injury to the somatosensory system can produce 'neuropathic' pain that lasts for months or years after any injury has healed (Treede, et al., 2008;Costigan, et al., 2009;Berger et al., 2011). This maladaptive 'disease of pain' has a 1.5-3% prevalence within the general population (Torrance, et al., 2006) and can associate with diabetic, postherpetic or HIV-related neuropathies, with multiple sclerosis or fibromyalgia as well as with traumatic nerve, spinal cord or brain injury (including stroke). It is associated with marked disruption of sensory signaling at the peripheral, spinal, thalamic and cortical levels (Sandkuhler, 2009;Zhuo, 2008;Patel and Dickenson, 2016;Chen, et al., 2014a;Pitcher and Henry, 2008). Afflicted individuals exhibit hyperalgesia, allodynia (the generation of a painful sensation by an innocuous stimulus) and bouts of stimulus-independent "electric shock like" pain (Mogil, 2009). Some experience causalgia (a persistent, burning pain).

Unfortunately, neuropathic pain is poorly responsive to opioid analgesics and this can lead to over-prescription and abuse. Even the "α2δ ligands", pregabalin (PGB) and gabapentin (GBP), which are first line treatments (Finnerup, et al., 2015) are not universally effective and as many as 65% of patients fail to report appreciable pain relief (Moore, et al., 2014). To better understand the mechanism of gabapentinoid action, we have addressed a paradox relating to their time course of action. Accepted animal models of neuropathic pain include experimental lesion of peripheral nerves such as sciatic chronic constriction (CCI) (Kim, et al., 1997;Mosconi and Kruger, 1996) or spared nerve injury (SNI) (Decosterd and Woolf, 2000). In such models, gabapentinoids attenuate hyperalgesia and/or allodynia within 30-60min of a parenteral injection (Hunter, et al., 1997;Kayser and Christensen, 2000;Field, et al., 2006;Kumar, et al., 2013;Alles and Smith, 2016;Luo, et al., 2002). Despite this, their reported actions on nociceptive neurons in

spinal cord or dorsal root ganglia (DRG) *in vitro* are 10-30 times slower; taking 10-15h to develop (Hendrich, et al., 2008;Hendrich, et al., 2012;Biggs, et al., 2014).

Alpha-2-delta (α2δ) refers to a family of accessory subunits that co-assemble with the pore forming α-subunits of high voltage-gated (HVA) Ca^{2+} channels (Dolphin, 2013;Dolphin, 2012;Zamponi, et al., 2015;Dolphin, 2016). One such subunit, α2δ-1 is upregulated in the DRG of animals subject to peripheral nerve injury and this coincides with the onset of signs of neuropathic pain (Luo, et al., 2001;Luo, et al., 2002;Bauer, et al., 2009). Pain behaviors also appear in animals genetically engineered to overexpress α2δ-1 (Li, et al., 2006;Li, et al., 2004). Gabapentinoids are transported into the neuronal cytoplasm, where they bind to α2δ-1 subunits (Gee, et al., 1996;Field, et al., 2006;Lana, et al., 2016;Field, et al., 2006;Hendrich, et al., 2008;Lana, et al., 2016). This interaction interferes with both the trafficking of α2δ–1 between the DRG cell body and primary afferent terminal (Bauer, et al., 2009) and the local trafficking of α2δ-1 subunits and their associated, pore forming α-subunits between the endoplasmic reticulum and the cell surface (Hendrich et al., 2008). Within nerve terminals, this impedes the ability of HVA-Ca^{2+} channels to interact with the vesicle fusion machinery for neurotransmitter release (Hoppa, et al., 2012). This leads to attenuation of synaptic transmission between nociceptive primary afferents and second order sensory neurons in the spinal dorsal horn (Hendrich, et al., 2012;Biggs, et al., 2014). It has been suggested that gabapentinoids antagonize the actions of the novel neurotrophin, thromospondin 4 which also binds α2δ (Pan, et al., 2016;Lana, et al., 2016).

Studies that failed to observe a rapidly developing, acute action of GBP *in vitro* (Moore, et al., 2002;Biggs, et al., 2014;Hendrich, et al., 2008) were done on dorsal horn neurons from naive animals rather than those subject to nerve injury. To the best of our knowledge, there are no studies of the acute antiallodynic action of gabapentinoids in the chronic constriction injury

(CCI) or spared nerve injury (SNI) model of neuropathic pain (Mosconi and Kruger, 1996;Decosterd and Woolf, 2000) that are correlated with changes in dorsal horn neurons. Furthermore, no attempts have been made to correlate the rapidly developing *in vivo* actions of GBP with acute changes in sensory processing at the level of the spinal cord or cortex.

We find, by studying neurons obtained *ex vivo* from animals that are responding to GBP, that the rapid time course of its *in vivo* anti-allodynic effect coincides temporally with altered synaptic transmission within the dorsal horn. Further analysis of rapidly developing GBP actions in *substantia gelatinosa ex vivo* suggest that i) they are mediated via an intracellular interaction, ii) they involve actions on the neurotransmitter release machinery iii) they involve differential effects on excitatory and inhibitory neurons.

It is possible that the GBP-induced increase in paw withdrawal threshold in nerve damaged animals (Hunter, et al., 1997;Kayser and Christensen, 2000;Field, et al., 2006;Kumar, et al., 2013;Alles and Smith, 2016;Luo, et al., 2002) is a simple reflection of attenuation of spinal withdrawal reflexes rather than the attenuation of pain *per se*. We therefore examined whether an acute behavioral drug response could be correlated with alterations in the response of the somatosensory cortex (S1) to vibrotactile stimulation (Potter, et al., 2016). S1 is a component of the "pain matrix" (Legrain, et al., 2011;Eto, et al., 2011). It is involved in processing sensory-discriminative aspects of both painful and non-painful touch (Komagata, et al., 2011). Structural changes in S1 neurons have been reported to correlate with chronic neuropathic pain states (Kim, et al., 2012). We found that vibrotactile stimulation of the limb ipsilateral to sciatic CCI produced robust S1 activation that was attenuated by the acute administration of GBP. A preliminary report of some of these findings has appeared (Alles, et al., 2015).

2. Materials and Methods

All animal experiments were approved by the University of Alberta Health Sciences Animal Welfare committee in accordance of the guidelines of the Canadian Council on Animal Care.

2.1 Surgery-Chronic Constriction Injury (CCI)

Fifty six male Sprague Dawley rats (21-23d) were subject to 7-10d chronic constriction injury (CCI) of the sciatic nerve (Mosconi and Kruger, 1996) as described previously (Balasubramanyan, et al., 2006). Briefly, the left sciatic nerve of rats under isoflurane anesthesia (5% induction, 2% maintenance) was exposed at mid-thigh level and two PE 90 polyethylene cuffs (ID 0.86 mm, OD 1.27 mm) were slit open on one side and gently attached around the sciatic nerve. The wound was closed with a silk suture, In the case of sham surgery, Forty six male rats (21-23d) were anesthetized under isoflurane and the sciatic nerve was exposed, but not touched with the forceps.

2.2 Surgery - Spared Nerve Injury (SNI)

Following isoflurane anesthesia as described above, eight male Sprague Dawley rats were subject to spared nerve injury (SNI) (Decosterd and Woolf, 2000;Pertin, et al., 2012). An incision was made through the *biceps femoris* to expose the sciatic nerve and the three terminal branches: the sural, common peroneal, and tibial The SNI procedure involved the ligation and transection of the common peroneal and tibial nerve, while leaving the third sural nerve intact Both the common peroneal and tibial nerves were tightly ligated with 5.0 silk and sectioned

approximately 5 mm distal to the ligation A 2-4mm segment was removed from the distal portion of the nerve stumps using care to avoid making unwanted contact with the sural nerve. Finally, the muscle and skin were closed in two layers, using sutures and wound clips, respectively

2.3 Behavioral Testing

Male Sprague-Dawley rats were tested for mechanical allodynia and hyperalgesia at 7-12 days after surgery (Fig 1a) using von Frey filaments of 1.4 g, 2 g, 4 g, 6 g, 10 g and 15 g weights. Animals were tested prior to and 30min after injection of 100mg/kg GBP or saline (Fig 1a). This dose is submaximal for the relief of inflammatory pain (Field, et al., 1997) and corresponds to the 90mg/kg dose which blocks ectopic nerve injury in nerve injured rats without effect on nerves from uninjured animals (Pan, et al., 1999). For testing, animals were placed in a plexiglass box with a wire-grid bottom, and pressure was applied to the mid-plantar area of the left paw (injured side) starting with a von Frey filament of the lowest weight (1.4 g) until it bent and then was held in this position for 2 seconds. This was performed 5 times and a positive result for each hair would be given if the animal withdrew its paw a minimum of 3 out of 5 times. If a negative result was obtained, the next heaviest filament would be used. A recovery period of at least 1 min between was allowed between successive filament applications. The paw withdrawal threshold (PWT) was calculated based on the weight of von Frey filament that elicited a positive result. Rats with a paw withdrawal threshold of 6 g or less were considered to be exhibiting mechanical allodynia (Balasubramanyan et al., 2006).

2.4 Preparation of acute spinal cord slices.

7-12 d after CCI or sham-surgery, animals were tested behaviourally for the presence of allodynia. Those exhibiting a PWT <6g received an IP injection of 100mg/kg GBP or control injection of saline. Following behavioural confirmation of an antiallodynic effect of GBP, animals were anesthetized with a large overdose of intra-peritoneal urethane (1.5 g/kg). Because animals developed allodynia at different rates and experiments were done on 6 animals per batch, it was possible to stagger electrophysiological analysis over a 5-6d period. This meant the youngest animals tested were 28d old (surgery at 21d, 7d to develop allodynia, tested immediately) and oldest were 40d (surgery at 23d, 12d to develop allodynia, tested 5d later).

Following anesthesia and the cessation of cardiac contraction and loss of ocular reflexes, the spinal cord was removed via laminectomy and transferred to partly-frozen, 'slushy' artificial cerebrospinal fluid (aCSF) containing (in mM): 118 NaCl, 2.5 KCl, 26 $NaHCO_3$, 1.3 $MgSO_4$, 1.2 NaH_2PO_4, 1.5 $CaCl_2$, 5 $MgCl_2$, and 25 D-glucose, 1 kynurenic acid. Which was continuously bubbled with carbogen (95% O_2, 5% CO_2). The L4-L7 region of the cord was glued with cyanoacrylate glue to a trapezoid-shaped block made out of 4% agar. Transverse slices (300 μm) were cut using a Microm HM 650V vibratome (Thermo Scientific, Waltham, MA, USA). Slices (6-8 per animal) were incubated in ~200mls aCSF (without kynurenic acid) at 37^{o}C for 1 hr prior to recording and then stored at room temperature (22-24^{o}C) for the remainder of the experimental day (Moran et al., 2004). Slices were thus examined between approximately 200 and 360min following euthanasia (Fig 1a). Recordings were made from the *substantia gelatinosa*, which was identified by its translucent appearance under IR-DIC (infrared-differential interference) optics and were made from the side ipsilateral to the sciatic injury. The

side ipsilateral to the nerve injury was marked by cutting a longer piece of agar along the desired side of the spinal cord after slicing was complete.

2.5 Calcium imaging of acutely isolated spinal cord slices.

During calcium imaging, slices were perfused at room temperature (22-24°C) with 95% O_2 - 5% CO_2 saturated aCSF containing (in mM): 127 NaCl, 2.5 KCl, 1.2 NaH_2PO_4, 26 $NaHCO_3$, 1.3 $MgSO_4$, 2.5 $CaCl_2$ and 25 *D*-glucose, pH 7.4. Acute spinal cord slices were imaged using a scanning confocal microscope (Olympus FV300) connected to an Argon laser (488 nm) for confocal (single-photon) imaging using a 20× objective (Olympus NA 1.0) and 2–3× optical zoom at full-frame (512 × 512 pixels). Neurons were visualized using the membrane-permeable Ca^{2+} indicator dye Fluo-4 acetoxymethyl ester (AM). An increase in Fluo-4 AM fluorescence intensity in response to laser excitation represented a Ca^{2+} rise. The acquisition speed was set at 1.08 frames per second.

Dorsal horn neurons were loaded with Fluo-4 AM by pressure injection (25-50 mmHg) using a broken patch electrode (outer tip diameter of 5-15 µm) at a depth of 50 µm The pressure injection was applied continuously for 20 min before a desired level of loading was achieved. Occasionally, more than one injection attempt was required. A desired level of loading was defined as at least 5 clearly visible dorsal horn cells and their basic morphology in a given field of view of 200-350 µm diameter.

Regions of interest (ROI) were drawn around individual cell bodies in the field of view and fluorescence traces were acquired using FluoView. The numerical values corresponding to the fluorescence traces were then exported to Microsoft Excel. Origin 2015 (Origin Lab Corp., Northampton, MA, USA) was used for measurement of normalized fluorescence ($(F_{max} - F_0)/F_0$) in response to stimulation with 35mM K^+. Finally, bar graphs were constructed in Origin 2015.

A one-way analysis of variance (ANOVA) with Bonferroni correction was used to calculate differences in $(F_{max} - F_0)/F_0$ between CCI and sham-operated animals that had received either GBP or saline.

2.6 In vivo Two-photon Cortical Imaging

This technique employs pressure injection of Ca^{2+}-indicator dyes directly into the somatosensory cortex of anesthetized rats to measure rises in intracellular Ca^{2+} of individual neurons in response to vibrotactile stimulation of the hind limb (Winship and Murphy, 2008). CCI or sham-operated rats (30-40 days old) were affixed to a stereotaxic frame. A surgical plane of anesthesia was achieved with 20% (w/v) urethane dissolved in saline and administered via intraperitoneal injection (1.25 g/kg; supplemented at 0.25 g/kg as needed). Body temperature was measured using a rectal probe and maintained at 37±0.5ºC. An incision was made along the medial portion of the scalp and the skin retracted to expose the skull. Bleeding from the scalp was electro-cauterized to prevent leaking onto the exposed surface of the skull. A 4 x 4 mm region of the skull overlying the right hemisphere somatosensory region was thinned to 25-50% of original thickness using a high-speed dental drill (~1.5-4.5mm lateral, +1.5 to -2.5 mm posterior to bregma). This thinned region was covered with 1.3% low-melt agarose dissolved in aCSF at 37 ºC containing in mM: NaCl 135, KCl 5.4, $MgCl_2.6H_2O$ 1, $CaCl_2.2H_2O$ 1.8, NaHEPES 5. The region was then covered with a 5mm glass coverslip. Hemodynamic intrinsic optical signal (IOS) imaging was performed through this thin skull preparation before *in vivo* Ca^{2+} imaging (Winship and Murphy, 2008). Imaging of intrinsic optical signals and local changes in blood flow using two-photon imaging have shown that blood flow to active areas of the cerebral cortex increases within 600 ms of the onset of neuronal activity (Winship, et al., 2007). For IOS imaging, the cortical surface was illuminated with a red LED (635nm). Reflected

light was captured in 12-bit format by a Dalsa Pantera 1M60 camera mounted on a Leica SP5 confocal microscope. The depth of focus was set between 200-300 μm below the cortical surface.

Custom-made piezo-electric mechanical bending actuators were used to elicit vibrotactile limb stimulation (1s, 200Hz) during IOS imaging (Winship and Murphy, 2008). A total of 40 trials of stimulation was performed on the hindlimb contralateral (cHL) to the cortex imaged and corresponding to the nerve-injured side. Placement of actuators was on the glabrous skin of the cHL, with consistent alignment relative to the flexion of wrist and ankle. Images were captured for 3.0s at 10 Hz (0.5s before and 2.5s after stimulus onset; inter-stimulus interval = 20s). The 40 trials were averaged in ImageJ software (NIH). Frames 1-1.5s after stimulus onset were averaged and divided by baseline frames 0.5s before stimulus onset to generate a hindlimb response map. The response map threshold was set at 50% maximal response, and overlaid on an image of surface vasculature to delineate the cHL somatosensory area (Fig 1b-f). These areas were subsequently used as guides for Ca^{2+} indicator injections (Winship and Murphy, 2008).

Subsequent to IOS imaging, the coverslip and agarose were removed. A metal plate was secured to the skull using cyanoacrylate glue and dental cement and then fastened to the surgical stage to prevent head movement. A 3 x 6 mm craniotomy was then performed centering over the cHL functional area, determined via IOS imaging. A dental drill was used to progressively thin the overlying skull until the bone could be removed with forceps, and the dura resected. The exposed cortical surface was bathed in saline. Pressure injections of membrane-permeant Oregon Green BAPTA-1 (OGB-1) were made 200-300μm below the cortical surface of the HL cortical region using glass micropipettes with resistances of 2-5 MΩ (Stosiek et al., 2003, Winship and Murphy, 2008). Alexa-594 was used as a tracer alongside OGB-1 to determine whether dye was

being successfully ejected from the micropipette tip. Multiple injections were performed until a desired level of loading was achieved. Typical loading is shown in Fig 1b. After OGB-1 injection, the cortex was incubated for 10 min with sulforhodamine 101 (SR101) dissolved in DMSO to label astrocytes (Winship and Murphy, 2008, Winship et al., 2007). The craniotomy was then covered with 1.3% agarose dissolved in aCSF and sealed with a glass coverslip.

Two-photon imaging was performed using a Leica SP5 MP confocal microscope equipped with a titanium-sapphire laser tuned to 810 nm for OGB-1 and SR101 excitation. A Leica HCX PL APO L 20x 1.0NA water immersion objective was used. Images were acquired using Leica LAS AF using two line-averages, a zoom of 1.7x and a frame-rate of 25 Hz. Images were acquired at 256 x 256 pixels over an area of 434 x 434μm, yielding a resolution of 1.7 μm per pixel. Ca^{2+} fluctuations in neurons and astrocytes were imaged at 130-180um below the cortical surface.

Using custom scripts written in NIH ImageJ, a median filter (radius, 1 pixel) was applied to each of the image sequences of 8 trial sweeps. The 8 filtered trails were then averaged to generate the final Ca^{2+} imaging frames to be analyzed. Regions of interest (ROIs) were drawn around visible neurons. Astrocytes were excluded from analysis by removing ROIs that co-labelled astrocytes in the SR101 channel. Numerical values representing raw neuronal fluorescence traces were exported from ImageJ and were imported into Microsoft Excel. A 5-point moving triangular smoothing filter was applied to each neuronal trace to increase signal-to-noise ratio. We found that this triangular filter did not affect the overall amplitude or main signal properties of our recorded Ca^{2+} traces, but did reduce single frame Ca^{2+} trace artifacts. $\Delta F/Fo$ traces were generated from the raw fluorescence traces as previously described (Winship and Murphy, 2008). Neuronal Ca^{2+} signals were exported from Microsoft Excel and analyzed in

Clampfit 9.0 (Molecular Devices, Silicon Valley, CA, USA). Due to the large number of signal traces that required analysis, various threshold criteria were tested to differentiate responsive from un-responsive neurons (Winship and Murphy, 2008). A threshold criterion requiring the neuronal Ca^{2+} fluorescence to increase by 3-times the standard deviation of the baseline period (baseline defined as 1s before stimulus onset), and remain above this criteria for 160ms (4 successive frames), was found to be optimal for separating responsive neurons from noise (Fig 1d). Neuronal traces that met these criteria were included in subsequent analysis.

The index of excitability used for cortical excitability was the 'neural mass' or the fraction of responsive cells multiplied by the mean normalized response (Doetsch, 2000, Erickson, 1986). This measure provided a more suitable parameter for comparing neuronal population coding and excitability of the PSC between different animals.

A one-way analysis of variance (ANOVA) with Bonferonni correction was used for comparing the neural mass between animals. Statistical significance was attributed if $p<0.05$.

2.7 Measurement of GBP Levels

21-30 day old Sprague-Dawley rats received either saline, 60 mg/kg GBP or 100 mg/kg GBP via intraperitoneal injection. After approximately 30 min, animals were anesthetized with a large overdose of intra-peritoneal urethane (1.5 g/kg) and spinal cords removed via laminectomy as described above. Whole brain was removed by making an incision along the midline of the head, peeling back the skin, cutting open the skull and dissecting out the brain.

Whole spinal cord or brain were frozen on solid CO_2 and stored in isopentane at -80^{o}C. Individual 300μm transverse spinal cord slices were prepared as described above from rats that had received 100mg/kg IP GBP 30min prior to euthanasia. They were subjected to the full

protocol slice preparation for electrophysiology (Fig 1a) prior to freezing on solid CO_2 and storage in isopentane for subsequent GBP measurement. All measurements were thus made from slices frozen approximately 155min following *in vivo* drug injection (Fig 1a).

At the time of analysis, samples were homogenized in ice cold methanol. For a standard control, 100 µl of the homogenate from saline-injected animal brain or spinal cord homogenate was used and for comparison, 100 µl of homogenate from GBP-injected animal brain or spinal cord homogenate was used in analysis. Samples were vortexed, placed on ice for 10 min and centrifuged at 10,000 *g* for 4 min. A calibration curve consisting of varying amounts of authentic GBP added to drug-free naive homogenates was run in parallel with each run.

The supernatant was transferred to a low volume silanized glass insert and 20µl of supernatant was injected onto the LCMS. Analysis was performed using a Waters ZQ Mass detector fitted with an ESCI Multi-Mode ionization source and coupled to a Waters 2695 Separations module (Waters, Milford, MA, USA). Mass Lynx 4.0 software was used for instrument control, data acquisition and processing. HPLC separation was performed on an Atlantis dC18 (3µm, 3.0 x 100mm) column (Waters, Milford, MA, USA) with a guard column of similar material. Mobile phase A consisted of 0.05% formic acid in water and mobile phase B was composed of 0.05% formic acid in acetonitrile. Initial conditions were 80% A and 20% B at a flow rate of 0.3ml/min. A gradient was run increasing to 80% B in 15 min followed by a return to initial conditions. The column heater and sample cooler were held at 30 ^{o}C and 4 ^{o}C respectively. Optimized positive electrospray parameters were as follows: capillary voltage 3.4kV; Rf lens voltage 1.0 V; source 110 ^{o}C; desolvation temperature 350 ^{o}C; cone gas flow (nitrogen) 100L/Hr; desolvation gas flow (nitrogen) 500 L/Hr. Cone voltage was held at 20 V.

Acquisition was done in the Single Ion Monitoring (SIM) mode and the mass:charge ratio was set at 171.2 to correspond to the molecular weight of GBP.

2.8 Electrophysiology

Acutely isolated spinal cord slices were superfused at room temperature (22-24°C) with 95% O_2 - 5% CO_2 saturated aCSF. The *substantia gelatinosae* were visualized under IR-DIC (infrared-differential interference) optics as a translucent band. Pipettes for recording had a resistance of 6-8 MΩ when filled with an internal solution that contained (in mM): 130 potassium gluconate, 1 $MgCl_2$, 2 $CaCl_2$, 10 HEPES, 10 EGTA, 4 Mg-ATP and 0.3 Na-GTP, pH 7.18-7.20, 290-300 mOsm.

An NPI SEC-05LX amplifier was used for recording in discontinuous, single electrode, current or voltage-clamp mode. Only data from neurons that produced a clear action potential overshoot of greater than 60 mV in amplitude were collected and data were collected from just one neuron per slice. Neurons were characterized on the basis of firing pattern in response to 800 ms depolarizing current pulses from a holding potential of -60 mV according to criteria in Balasubramanyan *et al.*, (2006) as either tonic, delay, phasic, transient or irregular. For measurement of excitability, current ramp commands were applied and discharge rates were analyzed as cumulative latency plots (Stemkowski and Smith, 2012). Current ramps were delivered at 33, 67, 100 or 133 pAs^{-1}. Only the 133 pAs^{-1} was used in analysis as this provided more discharge pattern data for comparison between cell types.

Spontaneous excitatory post-synaptic currents (sEPSCs),-were recorded at -70 mV. Miniature excitatory post-synaptic currents (mEPSCs), were recorded in the same way but in the presence of 1 µM TTX. All sEPSC and mEPSC were examined and visually accepted or rejected based on visual examination. Acceptable events had a sharp onset and exponential offset, a total

duration of <50 ms and an amplitude at least double the baseline noise. 3 min recordings were analyzed from each neuron.

2.9 Drugs and Chemicals

TTX was from Alomone Laboratories, Jerusalem, Israel. Kynurenic acid (Tocris) was from Cedarlane Laboratories (Hornby, Ontario, Canada). Gabapentin was from TTCI America, (Portland, Oregon, USA). Fluo-4 AM cell permeant, Oregon Green 488 Bapta-1 and sulforhodamine (SR-101) werefrom Molecular Probes, Invitrogen, Carlsbad, CA, USA. All other drugs and chemicals were from Sigma, St. Louis, MO, USA.

2.10 Data Analysis Software

All data and statistical analysis was performed using Origin 2015 (Origin Lab Corp., Northampton, MA, USA, www.originlab.com), except analysis of sEPSCs and mEPSCs which was performed using MiniAnalysis (Synaptosoft, Decatur, GA, USA, www.synaptosoft.com) and analysis of current ramp data which was performed using pCLAMP 8.0 (Molecular Devices Sunnyvale, CA, USA).

3. Results.

3.1 A single IP injection of GBP increases paw withdrawal threshold in neuropathic rats within 30 min.

We have shown previously that a single intraperitoneal injection of 100 mg/kg GBP in neuropathic CCI rats significantly increases the PWT within 30 min (Alles and Smith 2016). In confirmation of this, Fig 2a illustrates the increase in withdrawal threshold in rats subject to CCI

30min after IP injection of 100 mg/kg GBP (n=23) but not after injection of saline. Sham operated rats exhibited a withdrawal threshold of 15.0 ± 0.0 g after saline injection (n = 18) and this was unchanged in sham animals that had received GBP injection (15.0 ± 0.0, n=21).

One in 6 rats that underwent CCI surgery did not develop mechanical allodynia and these rats are called 'non-responders'. As another form of control for comparison to neuropathic rats, we performed experiments on non-responder rats and established that IP GBP did not have a significant effect on PWT compared to saline (Fig 2a).

We also confirmed that IP injection of 100mg/kg GBP rapidly attenuated allodynia (increased PWT) in 12 rats subject to spared nerve injury (SNI, Fig 2b). GBP did not affect PWT in sham operated rats (n=4). This model produces mechanical allodynia which persists for 30 weeks or more (Decosterd and Woolf, 2000) whereas that accompanying CCI abates within 20 weeks (Luo, et al., 2001).

3.2. Gabapentin administration reduces ex vivo dorsal horn excitability in rats subjected to CCI.

Rapid antiallodynic actions of GBP in nerve-injured rats *in vivo* have been associated with a decrease in glutamate release in the spinal dorsal horn (Coderre, et al., 2005). GBP would thus be expected to produce an overall decrease in excitability. To test this, we first examined the overall excitability of spinal cord slices obtained *ex vivo* from sham operated animals and those subject to CCI. Excitability was assessed by monitoring Ca^{2+} influx in response to depolarising 35mM K^+ challenges. In line with previous observations that CCI increases excitatory synaptic transmission and reduces inhibitory synaptic transmission in the spinal dorsal horn (Coull, et al., 2003;Balasubramanyan, et al., 2006) we found that slices from "neuropathic" animals subject to CCI were more excitable than those from sham operated animals ($p<0.001$ Fig. 2c). In other CCI

animals we administered GBP (100mg/kg IP) prior to euthanasia and the generation of spinal cord slices. This prior injection of GBP attenuated excitability of slices from neuropathic animals ($p<0.001$) whereas slices from sham operated animals were unaffected (Fig. 2c). Figure 2d illustrates superimposed sample recordings of K^+-evoked Ca^{2+} responses from 36 neurons in 3 spinal cord slices obtained from an animal that was injected with saline before euthanasia and generation of slices and responses of 34 neurons from another animal that had received 100mg/kg GBP. The black lines are averages of the illustrated records. Responses from GBP injected animals are smaller than those from saline injected animals.

3.3 GBP levels in spinal cord (whole cord and slices) and brain of IP injected animals

Levels of GBP peak in CNS tissues nwithin 1.5 h of intravenous injection or oral administration (Larsen, et al., 2016). We detected 1.89μg and 1.99μg of GBP per gram wet weight of spinal cord or brain respectively 45min after IP injection of 100mg/kg GBP. We also detected 0.55μg and 0.66μg of GBP per gram of spinal cord or brain respectively following IP injection of 60mg/kg GBP. The lack of effect of GBP on paw withdrawal threshold in sham operated animals is unlikely to reflect lack of penetration of the spinal cord and brain by GBP and may rather reflect an absence of effect on neurons from uninjured animals.

Generation of *ex vivo* spinal cord slices takes approximately 200 min following GBP injection (Fig 1a). For part of this time, slices are kept in a dissection solution at 37^{o}C for equilibration. We therefore tested whether the depression of dorsal horn excitability seen *ex vivo* following a prior *in vivo* injection could be attributed to the continued presence of GBP in the slices. This appeared to be the case as 0.54 ± 0.07μg/g, GBP was detected in slices from the

lumbo-sacral region of spinal cord neuropathic animals that had received 100 mg/kg GBP (n=12).

3.4 GBP has different effects on inhibitory versus excitatory neurons.

The spinal dorsal horn contains a variety of neuronal types which can be classified according to their morphology, neurotransmitter content and electrophysiological properties (Todd, 2010;Stebbing, et al., 2016). To an extent, morphology correlates with firing pattern and neurotransmitter content (Punnakkal, et al., 2014;Todd, 2010;Yasaka, et al., 2010). For example, neurons with an islet cell morphology are often GABAergic (Todd and Spike, 1993) and often display a tonic discharge pattern (Grudt and Perl, 2002;Labrakakis, et al., 2009). Neurons with a "delay" firing pattern are often excitatory (Punnakkal, et al., 2014). We have demonstrated that long term (4-5d) exposure of dorsal horn neurons in organotypic culture to gabapentinoids is more effective in inhibiting excitatory synaptic drive to putative excitatory delay firing neurons than to putative inhibitory tonic firing neurons (Biggs et al 2014). To determine whether IP GBP has similar, yet rapidly developing, differential effects on input to excitatory versus inhibitory neurons, we examined its *ex vivo* effects on spontaneous synaptic transmission in tonic neurons and in delay firing neurons. Neurons were classified according to firing pattern using criteria defined in our previous work (Balasubramanyan et al., 2006). In a sample of 122 neurons, we found 36% tonic, 27% delay, 20.5% transient, 12.5% phasic and 4% irregular firing.

3.4.1. Effects of GBP on sEPSCs in Delay Neurons. Fig 3a illustrates the typical discharge pattern of a putative excitatory delay neuron. Prior injection of 100mg/kg GBP reduced average sEPSC amplitude in delay neurons from 26±2.4pA (n=7 neurons in 7 slices) to 23±3.3pA (n=6 neurons in 6 slices; $p<0.05$). The reduction in sEPSCs amplitude in rats that had received GBP and those had received saline is illustrated in a cumulative probability plot (Fig

3b) where *p<0.001,* (K-S test). GBP also reduced average sEPSC frequency (increased interevent interval, IEI) from 905+62ms (n=7) to 1435±81ms (n=6, *p<0.05).* Plotting the data as a cumulative probability plot (Fig 3c) yielded *p<0.001* (KS statistics).

3.4.2. Effects of GBP on sEPSCs in Tonic Neurons. Figure 3d illustrates the typical discharge pattern of a putative inhibitory tonic neuron. By contrast with its action on delay neurons, GBP did not reduce sEPSC amplitude in tonic neurons (25±8.4pA, n=10 in saline injected animals, 25±4.5pA in GBP injected animals n=11, p>0.05). GBP also increased the frequency (decreased the interevent interval) from 4839±456ms (n=10) to 3015±205ms (n=11, *p <0.05*). Cumulative probability plots for the action of GBP on the amplitude and interevent interval of sEPSCs in tonic neurons are shown in Fig 3e and f. The decrease in interevent interval is significant (*p<0.001* KS test; Fig 3f).

3.4.3. Effects of GBP on sEPSCs inTransient Neurons. At least in mice, recent evidence suggests that many transient firing neurons display an excitatory phenotype (Punnakkal et al 2014). We therefore examined the effect of GBP injection on their excitatory synaptic drive and found that transient neurons were affected in the same way as putative excitatory delay neurons. Fig 3g illustrates the typical discharge pattern of a transient neuron; threshold is characteristically high and no more than a single action potential can be generated regardless of intensity of depolarizing current.

Prior injection of 100mg/kg GBP reduced sEPSC amplitude in transient neurons from animals subject to CCI from 25±2.7pA (n=7) to 22±2.8pA (n=7) (*p<0.*001). The difference between sEPSCs amplitudes in transient neurons from rats that had received GBP and those had received saline is illustrated in a cumulative probability plot (Fig 3h) where *p<0.001,* (K-S test). GBP also reduced average sEPSC frequency (increased interevent interval) from 1522±167ms

(n=7) to 2220±217 1ms (n=7, $p<0.01$). Plotting the data as a cumulative probability plot (Fig 3i) yielded $p<0.02$ (KS statistics).

3.5 Which actions of GBP are a consequence of nerve injury?

To determine which of the above described actions of GBP are contingent on nerve injury we also examined its actions on sEPSC in delay, tonic and transient neurons from sham operated animals.

In delay neurons, GBP reduced sEPSC amplitude in sham operated animals in a similar fashion to its action on neurons from animals subject to CCI (Fig 3b and Fig 4a). By contrast, GBP did not affect interevent interval in neurons from sham operated animals (Fig 4b). This differs from its aforementioned action in delay neurons from animals subject to CCI where interevent interval is increased (Fig 3c).

GBP did not affect sEPSC amplitude in tonic neurons from sham operated animals and this corresponds with its overall lack of effect on sEPSC amplitude in tonic neurons from animals subject to CCI (Figs 4c and 3e). The drug reduced sEPSC frequency (increased interevent interval) in sham operated animals. This contrasted with GBP's aforementioned action on tonic neurons from animals subject to CCI where frequency was increased (Fig 4d compared with Fig 3f).

In transient neurons, GBP reduced sEPSC amplitude in sham operated neurons in a similar fashion to its action on transient neurons from animals subject to CCI (Fig 4e and Fig 3h). By contrast, interevent interval was unchanged in transient neurons from sham operated animals but was increased in neurons from animals subject to CCI (Fig 4f compared to Fig 3i).

From this, we can make the interim conclusion that the effects of GBP to increase interevent interval (reduce sEPSC frequency) in excitatory delay and transient neurons after CCI

(Fig 3c and i) and its ability to decrease interevent interval (increase sEPSC frequency) in inhibitory tonic cells after CCI (Fig 3f), are most pertinent to understanding its anti-allodynic actions. Because GBP exerts similar effects on sEPSC amplitude in delay and transient cells from sham operated and animals subject to CCI (Figs 3b and 4a; 3h and 4e), these effects may have little relevance to its antiallodynic action.

Effects of GBP on tonic, delay and transient neurons from sham operated and CCI animals are summarized in Table 1.

3.6. Effects of GBP on mEPSCs

Since GBP decreased sEPSC frequency in delay neurons (Fig 3c and 3i) and increased it in tonic neurons (Fig 3f) we determined whether IP GBP had differential effects on the neurotransmitter release process independent of depolarization-induced Ca^{2+} influx by examining its effects on mEPSCs.

3.6.1. Effects of GBP on mEPSC's in delay neurons. For delay neurons from animals subject to CCI, the effects of IP GBP on mEPSCs were similar to those on sEPSCs. Average mEPSC amplitude in neurons from saline injected animals was 25.6±0.3 pA (n=7) and this compared with 18.9±0.3 pA (n=5) in delay neurons from GBP injected animals (*P<0.001*). Average interevent interval was significantly increased (*p<0.01*) from 1947±225ms (n=7) to 2873±171ms (n= 5). Similar differences were seen from cumulative probability plots where GBP reduced mEPSC amplitude (*p<0.001,* K-S test, (Fig 5a) and increased interevent interval (*p<0.002*, K-S test, Fig 5b). To provide further information about the effects of GBP on mEPSC amplitude, we separated events into 5pA bins and displayed the amplitude data as a frequency histogram (Fig 5c). GBP increased the number of small events and decreased the number of small events.

3.6.2,. Effects of GBP on mEPSC's in tonic neurons The effect of GBP on mEPSCs in this population did not at all correspond with its actions on sEPSCs (compare Figs 5d and 5e with Figs 3e and f). GBP thus increased mEPSC amplitude (Fig 5d, $P< 0.005$ KS test) but had no effect on mEPSC interevent interval (Fig 5e). Average mEPSC amplitude in neurons from saline injected animals was 22.8±0.9 pA (n=5) and this was less than the value of 28.1±1.6 pA (n=10) in tonic neurons from GBP injected animals ($p<0.02$), Interevent interval was not significantly changed ($p>0.05$). In tonic neurons from saline injected animals interevent interval was 4808±437ms (n=5) compared to 5113±433ms in neurons from GBP injected animals. Further analysis of the effects of GBP by means of a frequency histogram of binned event amplitudes suggested that the drug increased the amplitude of large events but reduced the amplitude of small events (Fig 5f).

Since transient firing neurons were encountered less frequently than tonic or delay firing neurons, the limited number of recordings of mEPSCs we obtained from this population precluded meaningful analysis of the data.

3.7. Effects of GBP on Intrinsic Neuronal Properties.

To determine whether IP GBP produces differential effects on the intrinsic neuronal properties of putative excitatory delay and putative inhibitory tonic neurons, we studied the cumulative latency of action potentials in response to depolarizing current ramps (Fig 5g and 5h). GBP injection increased cumulative latency of APs in delay firing neurons in animals subject to CCI (Fig 5i, $p<0.005$). Although it did not affect cumulative AP latency in tonic neurons (Fig 5j, p>0.05, one-way ANOVA), GBP did appear to affect the variance in latency of APs. Note that error bars on data from GBP treated neurons are smaller than controls. It may

therefore exhibit some subtle action on spike frequency adaptation in a subpopulation of tonic neurons.

3.8. GBP reduces Primary Somatosensory Cortex (S1) Excitability in Neuropathic Rats.

It may be argued that the observed actions of GBP on PWT in animals subject to CCI (Fig 2a and b) and the corresponding changes in synaptic transmission in *substantia gelatinosa* (Figs 3-) simply reflect depression of spinal reflexes rather than suppression of pain *per se*. Therefore, in order to determine whether the acute actions of GBP impact a higher level of somatosensory processing, we examined the effect of IP GBP on excitability of the primary somatosensory cortex (S1).

As an index for overall network excitability in S1, we calculated the 'neural mass' (fraction of responsive neurons $\times$ mean dF/F_0, see Methods) before and 10 min following IP GBP injection. To ensure that Ca^{2+} signals were recorded from neurons, we loaded superficial layers of the cortex via bath application of sulforhodamine-101 (SR-101), which is preferentially taken up by glia (astrocytes). By excluding all SR-101-loaded cells, we assumed that the remainder of the Ca^{2+} signal was neuronal (Fig 6a). Fig 6b illustrates the averaged response of 114 neurons in S1 to vibrotactile stimulation of the limb that was subject to CCI.

As expected, before GBP administration, the neural mass of neuropathic CCI rats was significantly higher than in sham-operated rats (i.e. S1 was hyperexcitable; $P<0.05$, one-way ANOVA with Bonferroni correction. Fig 6c). Within 10 minutes of injection, 100 mg/kg IP GBP significantly reduced neural mass in neuropathic CCI rats by approximately 56% ($P<0.05$, one-way ANOVA with Bonferroni correction Fig 6c). However, neural mass in sham rats was not significantly affected ($P>0.05$, one-way ANOVA) 10 min following GBP injection.

4. Discussion

We confirmed that GBP increases PWT within 30 min of IP injection in CCI and SNI neuropathic rats as has been reported in other pain models (Hunter, et al., 1997;Field, et al., 2006;Kumar, et al., 2013) and in our previous publication (Alles and Smith, 2016). We now show that this effect in CCI rats correlates temporally with an overall decrease in excitability of dorsal horn and primary somatosensory cortex. Within *substantia gelatinosa,,* effects of GBP correspond to a decrease in excitatory drive to putative excitatory neurons.

From studies in hippocampal neurons, Hoppa *et al* (2012) posited that α2δ subunits function through two mechanisms. "A trafficking step from the cell soma and a local step at the presynaptic terminal allowing synapses to have increased exocytosis with decreased Ca^{2+} influx". We suggest that when α2δ1 levels are elevated, either in neuropathic pain models or by genetic modulation (Luo, et al., 2002;Luo, et al., 2001;Bauer, et al., 2009), it is rapidly and locally trafficked from the endoplasmic reticulum to the plasma membrane of primary afferent nerve terminals. This process is interrupted by gabapentinoids within 30min of intraperitoneal injection and accounts for the rapid actions we observe in *ex vivo substantia gelatinosa* (Figs 3-5). By contrast, in the uninjured situation, the level α2δ1 in at neurotransmitter release sites is governed by slower trafficking from the cell bodies to primary afferent terminals (Bauer, et al., 2009). In this situation, a slower action of gabapentinoids represents the gradual depletion of α2δ1 at nerve terminals over periods of several days as they do not appear to affect endocytosis (Bauer, et al., 2009). This may account for the slowly developing effects observed in previous *in vitro* studies (Biggs, et al., 2015;Biggs, et al., 2014)

4.1. An intracellular site of in vivo GBP action.

Long-term actions of GBP *in vitro* require its transport into the cytoplasm via the neutral aminoacid transporter (Biggs et al., 2014: Hendrich et al 2008). We suggest that rapidly developing *in vivo* effects are also mediated via an intracellular action with α2δ1. This is because drug actions in *substantia gelatinosa* persist *ex-vivo* (Figs 3-5) and GBP can be detected in spinal cord slices after their removal from animals that were displkaying an anti-allodynic response to the drug. GBP is not particularly lipophilic, so it is unlikely that its persistence in the tissue reflects non-specific binding to cell membranes. The K_D for GBP binding to α2δ−1 is in the 100nM range (Kadurin, et al., 2016;Lana, et al., 2016). Assuming a diffusion-limited association rate constant of 10^6 to 10^8 per molar per second, the average bound time for a single molecule of GBP would lie between 1 and 100 seconds. Since the slices (6-8 per animal) are incubated in a relatively large volume of CSF (~200ml) for 60 min or more, it is very unlikely GBP remains bound to an extracellular site on α2δ−1 and more probable that intracellular retention accounts for our observations These observations are congruent with those of Lana et al (2016) who showed that GBP displacement of thrombospondin 4 binding is effected at an intracellular site on α2δ−1.

4.2. GBP has differential actions on excitatory compared to inhibitory neurons

In general, GBP decreases excitatory drive to putative excitatory neurons but has weaker and more complex actions on excitatory drive to putative inhibitory neurons (Table 1). This fits with the observation that its rapid actions are associated with an overall decrease in excitability of spinal cord slices from nerve injured animals (Fig 2c and d). It is also consistent with the finding that glutamate release is decreased *in vivo* in nerve injured animals (Coderre et al., 2005)

and that GBP has little effect on GABA/glycine mediated mIPSCs in deep dorsal horn (Zhou and Luo, 2015). Our analysis of *ex vivo* GBP actions were confined to effect on spontaneous synaptic activity as the amplitudes of EPSCs evoked by dorsal root stimulation are highly variable (Lu and Perl, 2005;Biggs, et al., 2014) and this precludes statistical comparison of GBP effectiveness from sham operated and CCI animals. Although this means we cannot distinguish between synaptic activity from primary afferents and that from other excitatory interneurons this may have little bearing on the ability of GBP to damp down overall dorsal horn excitability.

4.3. Effects of GBP on putative excitatory delay and transient neurons.

We have defined excitatory neurons on the basis of the initial delay in action potential discharge by depolarizing current pulses (Fig 3a). It should be noted that in a detailed morphological and electrophysiological study of lamina II neurons, the delayed firing pattern was only ever seen in excitatory neurons that were identified by the presence of VGLUT2 (vesicular glutamate transporter 2) immunoreactivity (Yasaka, et al., 2010). GBP reduced the amplitude of sEPSCs in putative excitatory delay neurons from animals subject to CCI (Fig 3b). It is not known whether this action is α2δ-1-dependent as it was also seen in sham operated animals (Fig 4a; Table 1). Decreased sEPSC amplitude may be a consequence of decreased mEPSC amplitude (Fig 5a). Because GBP increased the number of small mEPSC events while decreasing the number of large events (Fig 5c) this suggests the drug acts presynaptically to reduce quantal size or quantal content or both. The GBP-induced increase in IEI (decrease in frequency) of sEPSCs in delay neurons (Fig 3c) is not seen in sham operated animals, (Fig 4b) but corresponds to a decrease in mEPSC frequency (Fig 5b) and presumably to a presynaptic site of action that appears only in neuropathic animals.

Although we do not have mEPSC data for GBP actions on putative excitatory transient neurons, effects on sEPSC's exactly parallel those seen in delay neurons (Table 1). The amplitude of sEPSC's is thus reduced in both sham operated animals and those subject to CCI (Figs 3h and 4e). Interevent interval is only increased in animals subject to CCI (Fig 3i) and not in shams (Fig 4f).

Taken together, the data from transient and delay neurons suggest that a presynaptic action to attenuate release of glutamate onto putative excitatory neurons may play a major role in GBP-induced decrease in dorsal horn excitability in neuropathic animals as suggested by Coderre et al (2005).

4.4. Effects of GBP on putative inhibitory tonic neurons.

Yasaka *et al* (2010) identified 23 inhibitory neurons in rat lamina II by the presence of immunoreactivity for the vesicular GABA transporter (VGAT). All but 2 of these cells exhibited a tonic firing pattern. We therefore used the presence of a tonic firing pattern to identify inhibitory neurons. GBP slightly increased the amplitude of mEPSCs in putative inhibitory tonic neurons in CCI animals (Fig 5d). This is unlikely to reflect a postsynaptic effect as sEPSC amplitude was unchanged (Fig 3e; Fig 4c; Table 1). It may rather reflect a presynaptic action such that the amplitude of large events is increased whereas that of small events is decreased (Fig 5c). Regardless of the mechanism, an increase in mEPSC amplitude that is not reflected as a change sEPSC amplitude is unlikely to contribute to the overall depressant and antiallodynic actions of GBP.

GBP decreased the frequency (increased the interevent interval) of sEPSC in tonic neurons from sham operated animals (Fig 4d), did not affect mEPSC frequency in CCI animals (Fig 5e) yet did increase sEPSC frequency (Fig 3f). Since tonic firing cells are usually inhibitory

(Yasaka, et al., 2010), this latter effect is consistent with an overall decrease in *substantia gelatinosa* excitability (Fig 2c and d). The underlying mechanism is however difficult to explain.

4.5. GBP's effect on intrinsic neuronal excitability of substantia gelatinosa neurons.

The *ex vivo* data presented in Figure 5i and j suggest that IP GBP has a differential but rather weak effects on the excitability of delay and tonic neurons. In the first case, latency to action potential discharge is increased. This suggests that delay neurons, which are mostly excitatory (Punnakkal, et al., 2014;Yasaka, et al., 2010) will require a longer depolarizing stimulus to generate an action potentials after GBP injection. In tonic, putative inhibitory neurons, GBP reduces the cell to cell variability in cumulative latency of AP generation. It remains to be determined whether these actions contribute to the overall decrease in excitability seen with GBP (Fig 2c and d).

4.6. GBP and nociceptive processing at the level of the somatosensory cortex

We can never really know to what extent the effects of GBP in animals models represent the antiallodynic and pain-suppressing effects observed in the clinical situation. Recent evidence suggests that gabapentinoids may be effective in operant models which require cortical processing of noxious stimulation (Harte, et al., 2016). The emotional experience of pain involves a complex system of neural structures in the brainstem reticular formation and the limbic system One such neural structure involved in affective pain processing involves the anterior cingulate cortex (ACC) (Chen, et al., 2014b;Zhuo, 2008;Chen, et al., 2014a). Unfortunately, for our studies these structures are too deep (>500 μm) to easily image using two-photon laser scanning microscopy. However, imaging in layer II/III of S1 showed that IP gabapentin rapidly depressed the activity generated by a vibrotactile stimulus (Fig 6). This suggests that somatosensory activation resulting from processing of peripherally generated

cutaneous and proprioceptive information is elevated in untreated animals after CCI, thereby leading to hyperexcitability of S1, and that this hyperexcitability is reversed by GBP. This may relate to the drugs anti-allodynic action.

Since GBP exerts inhibitory actions on synaptic transmission in anterior cingulate cortex (Chen, et al., 2014b), it remains to be determined whether the effects of GBP seen in S1 cortex *in vivo* (Fig 6) reflect a direct action on cortical networks, and/or whether they are an "upstream" consequence of inhibition at the spinal and/or thalamic level. In support of effects of gabapentinoids on pain processing in subcortical structures, it has recently been shown that pregabalin exerts actions on sensory processing in the ventral posterior thalamus of neuropathic animals (Patel and Dickenson, 2016).

Our data are consistent with the idea that levels of α2δ protein dictate the *rapidity* of gabapentinoid action (Alles and Smith, 2016), and this involves an intracellular action to reduce glutamate release from excitatory terminals onto excitatory neurons. In addition, they provide a hypothesis for understanding the slow rate of onset of gabapentinoid effect in the clinic where drug effects take several days to develop (Sharma, et al., 2010). In a spinal nerve ligation model of neuropathic pain, α2δ1 levels are elevated at 2-4 weeks but return to pre-injury levels with time (Luo et al, 2001). If a similar situation occurs in patients and α2δ1 levels decrease with time despite the chronic persistence of neuropathic pain, a slowly developing action of GBP may be predicted (Alles and Smith, 2016).

Figure Legends

Figure 1. Time course of *ex vivo* spinal cord experiments and procedure for *in vivo* imaging of rat cortex. a. Time course of experiments for investigating the anti-allodynic actions of GBP in *ex vivo* spinal cord. Adult maleSprague-Dawley rats were subject to CCI surgery and developed signs of neuropathic pain within 7 days as shown by a reduction in paw withdrawal threshold (PWT). Sham-operated rats were used as controls. On a given day of experiments, a rat's PWT was recorded before and after IP injection of 100 mg/kg IP GBP or saline (control). Following anesthesia, the spinal cord was removed and transverse 300 μm slices of lumbar cord prepared for Ca^{2+} imaging or electrophysiological analysis. **b.** low power image (field of view diameter = 12 mm) of thinned skull cortical preparation; red outline shows threshold area responding to contralateral hindlimb (cHL) stimulation (width approximately 1-2 mm) as measured by hemodynamic IOS imaging. **c.** 0.5s averaged IOS image of the same field of view as **c** prior to stimulation. **d.** Averaged IOS signal obtained during 1s 200 Hz vibrotactile stimulation of the cHL to allow generation of a 'somatosensory map **e**. average of 1s IOS post stimulus. **f.** Typical loading (false colour) of the cortex with OGB-1 (Ca^{2+} indicator) and with Alexa-594 (tracer) following injection into the cortex up to a depth of 300 μm.

.

Figure 2. Acute anti-allodynic actions of GBP and cellular correlates in the dorsal horn. **a.** A single intraperitoneal injection of 100 mg/kg GBP significantly increased PWTs within 30 min in neuropathic CCI rats with no effect in non-responder rats that failed to develop allodynia following CCI. For saline injected controls n=22, for GBP injected n=23, for non-responders, saline injected n=6, for non-responders GBP injected n=6.). *One-way ANOVA with

Bonferroni correction, $p < 0.05$. **b.** Time course of effects of 100mg/kg on PWT of rats subject to spared nerve injury (SNI). Upward arrows indicate times of single IP injections of drug, PWT was measured 30min after injection PWT in sham operated animals was unchanged (n=4, grey half filled circles). **c.** Effect of IP GBP injection on dorsal horn excitability (Ca^{2+} response to 35mM K^+) in neuropathic CCI versus sham-operated rats. Prior IP GBP reduces dorsal horn excitability in CCI, but not sham-operated rats. The dorsal horn excitability of CCI rats was higher than sham-operated rats. Controls for sham and CCI rats were injected with IP saline. All experiments were performed blinded to the treatment of each rat until after analysis. CCI GBP, n = 4 rats, 12 slices, 107 cells; CCI (Saline Control), n = 3 rats, 8 slices, 80 cells; Sham GBP, n = 3 rats, 11 slices, 79 cells; Sham (Saline control) n = 3 rats, 10 slices, 105 cells. *One-way ANOVA with Bonferroni correction, $p < 0.05$. Data in **a,b** and **c** are presented as mean ± SEM. **d.** Raw fluorescence traces comparing the average of 35 mM K^+-evoked Ca^{2+} responses in a saline-injected (top) compared to GBP-injected (bottom) CCI neuropathic rat. Prior GBP injection produces a noticeable reduction in the average amplitude of the response compared to prior saline injection as shown by the black line in each case (n=33 neurons for control CCI trace, n=26 for GBP injected). Calibration bar in arbitrary fluorescence units (AU) refers to both sets of traces.

Figure 3. Neuron Types and Effects of Prior GBP Injection on sEPSC's in Animals Subject to CCI. a, d and **g.** Sample recordings of AP discharge in delay, tonic and transient neurons in response to two different depolarising current steps. Neuronal RMP was are held at -60 mV prior to current injection. **b** and **c.** sEPSC amplitude and inter-event interval (IEI) of putative

excitatory delay neurons from CCI rats. n's for GBP-injected = 6 neurons/slices, 6 rats, 753 events. n's for Saline-injected = 7 neurons/slices, 7 rats, 1188 events. $p<0.0001$ for both amplitude and IEI). **e** and **f.** sEPSC amplitude and inter-event interval of putative inhibitory tonic neurons from CCI rats. n's for GBP-injected = 11 neurons/slices, 10 rats, 636 events. n's for saline-injected = 10 neurons/slices, 7 rats, 397 events. ($p>0.05$ for amplitude and $p<0.00005$ for IEI). **h.** and **i.** sEPSC amplitude and IEI of putative excitatory transient neurons from CCI rats. n's for GBP-injected = 7 neurons/slices, 5 rats, 685 events. n's for saline-injected = 7 neurons/slices, 7 rats, 859 events. For amplitude $p<0.0001$ and for IEI $p<0.02$). Cumulative probability plots were compared with the Kolmogorov-Smirnov test and statistical significance was attributed if $p<0.05$.

Figure 4. Effects of prior GBP injection on *substantia gelatinosa* neurons recorded *ex vivo* from sham operated rats. a. sEPSC amplitude and **b.** inter-event interval (IEI) of putative excitatory delay neurons from sham-operated rats. n's for GBP-injected = 7 neurons/slices, 5 rats, 99 events. n's for Saline-injected = 5 neurons/slices, 5 rats, 98 events. ($p<0.00001$ for amplitude and $p>0.05$ for IEI). **c.** sEPSC amplitude and **d.** inter-event interval (IEI) of putative inhibitory tonic neurons from sham-operated rats. n's for GBP-injected = 5 neurons/slices, 5 rats, 121 events. n's for Saline-injected = 7 neurons/slices, 5 rats, 315 events. ($p>0.05$ for amplitude and $p<0.007$ for IEI). **e.** sEPSC amplitude and **f.** inter-event interval (IEI) of putative excitatory transient neurons from sham-operated rats. n's for GBP-injected = 4 neurons/slices, 4 rats, 226 events. n's for Saline-injected = 3 neurons/slices, 2 rats, 176 events. ($p<0.0007$ for amplitude and $p>0.05$ for IEI). Cumulative probability plots were compared with the Kolmogorov-Smirnov test and statistical significance was attributed if $p<0.05$.

Figure 5. Effects of prior GBP injection on the neurotransmitter release process (mEPSC) and intrinsic neuronal excitability of *substantia gelatinosa* neurons recorded *ex vivo* from CCI rats .a. mEPSC amplitude and **b.** inter-event interval (IEI) of putative excitatory delay neurons from CCI rats. n's for GBP-injected = 5 neurons/slices, 4 rats, 281 events. n's for saline-injected = 7 neurons/slices, 4 rats, 580 events. ($p<0.000001$ for amplitude and $p<0.002$ for IEI). **c.** Delay neuron mEPSC amplitude data re plotted as frequency histogram (bin width = 5pA). **d.** mEPSC amplitude and **e.** inter-event interval (IEI) of putative inhibitory tonic neurons from CCI rats. n's for GBP-injected = 10 neurons/slices, 7 rats, 322 events. n's for saline-injected = 5 neurons/slices, 3 rats, 172 events. ($p<0.005$ for amplitude and $p>0.05$ for IEI). **f.** Tonic neuron mEPSC amplitude data re plotted as frequency histogram (bin width = 5pA). **g-j** Measurement of intrinsic neuronal excitability. Depolarising current ramp command bottom) and AP firing pattern (top) associated with **g.** a typical delay firing neurons and **h.** a typical tonic firing neurons of the *substantia gelatinosa***. i.** cumulative latency to AP discharge is increased ($p<0.005$) in putative excitatory delay neurons in GBP compared to saline-injected CCI rats. n's for GBP-injected = 7 neurons/slices, 6 rats. n's for saline-injected = 9 neurons/slices, 7 rats. **j.** In tonic neurons, cumulative latency for AP discharge is not significantly affected in GBP- compared to saline-injected CCI rats. n's for GBP-injected = 13 neurons/slices, 11 rats. n's for saline-injected = 12 neurons/slices, 11 rats. 133 pAs-1 current ramp was used to plot cumulative latency versus AP spike number in each case. Cumulative latency plots were compared by one-way ANOVA with Bonferroni correction and statistical significance was attributed if $p<0.05$.

Figure 6. *In vivo* primary somatosensory cortical imaging in neuropathic CCI rats.

a. Loading of glial (red, left) and neuronal (green, right) cells at 100 μm depth in the primary somatosensory cortex of adult male rats for *in vivo* two-photon imaging. Glial cells are loaded by bath application of sulforhodamine and neuronal cells via pressure injection with Ca^{2+} indicator OGB-1 AM dye. **b.** Recording of responses using *in vivo* cortical two-photon Ca^{2+} imaging. Averaged normalized Ca^{2+} rise (shown in red) of a neuronal cell in response to repeated vibrotactile stimulation (onset at 2s, duration of 1s) of the injury-side hindpaw at 200 Hz. Sampling time = 40ms/frame, grey lines averaged data records from 9 neurons, black line is average of average from 114 neurons (some non-responders) **c.** *In vivo* primary somatosensory cortical imaging in neuropathic CCI rats immediately following IP GBP. 100 mg/kg intraperitoneal GBP injection reduced cortical excitability (neural mass) in neuropathic CCI (n=3 rats) within 10 min of injection, with no significant reduction observed in sham-operated rats (n=2 rats). A reduction in cortical excitability was observed in sham-operated rats at 20 min post-injection with no further reduction observed in neuropathic rats compared to 10 min post-injection. At 30 min post-injection there were no significant differences compared to at 20 min post-injection in cortical excitability of either CCI or sham-operated rats. *$p<0.05$, one-way ANOVA with Bonferroni correction. All data are presented as mean ± SEM.

	ACUTE EFFECT OF IP GBP ON SHAM OPERATED ANIMALS	ACUTE EFFECT OF IP GBP ON ANIMALS SUBJECT TO CCI
DELAY NEURONS		
sEPSC AMPLITUDE	↓	↓
sEPSC IEI	NO EFFECT	↑
mEPSC AMPLITUDE	Not Determined	↓
mEPSC IEI	Not Determined	↑
TRANSIENT NEURONS		
sEPSC AMPLITUDE	↓	↓
sEPSC IEI	NO EFFECT	↑
mEPSC AMPLITUDE	Not Determined	Not Determined
mEPSC IEI	Not Determined	Not Determined
TONIC NEURONS		
sEPSC AMPLITUDE	NO EFFECT	NO EFFECT
sEPSC IEI	↑	↓
mEPSC AMPLITUDE	Not Determined	↑
mEPSC IEI	Not Determined	NO EFFECT

Table 1 Summary of actions of prior IP injection of 100mg/kg GBP on *ex vivo* properties of sEPSC's and mEPSC's in *substantia gelatinosa* neurons.

Reference List

Alles SR and Smith PA (2016) The Anti-Allodynic Gabapentinoids: Myths, Paradoxes, and Acute Effects. *Neuroscientist*DOI: 10.1177/1073858416628793.

Alles SRA, Bukhanova N, Bandet M, Winship IR and Smith PA (2015) Peripheral Nerve Injury Promotes Emergence of Acute, Neuron-type-specific Depressant Actions of Gabapentin in *Substantia Gelatinosa* and Primary Somatosensory Cortex. *Neuroscience 2015 Abstracts Chicago, IL: Society for Neuroscience, 2015 Online*Program No. 210.20.

Balasubramanyan S, Stemkowski PL, Stebbing MJ and Smith PA (2006) Sciatic Chronic Constriction Injury Produces Cell-type Specific Changes in the Electrophysiological Properties of Rat *Substantia Gelatinosa* Neurons. *J Neurophysiol* **96**:579-590.

Bauer CS, Nieto-Rostro M, Rahman W, Tran-Van-Minh A, Ferron L, Douglas L, Kadurin I, Sri Ranjan Y, Fernandez-Alacid L, Millar NS, Dickenson AH, Lujan R and Dolphin AC (2009) The Increased Trafficking of the Calcium Channel Subunit {alpha}2{delta}-1 to Presynaptic Terminals in Neuropathic Pain Is Inhibited by the {alpha}2{delta} Ligand Pregabalin. *Journal of Neuroscience* **29**:4076-4088.

Berger JV, Knaepen L, Janssen SPM, Jaken RJP, Marcus MAE, Joosten EAJ and Deumens R (2011) Cellular and molecular insights into neuropathy-induced pain hypersensitivity for mechanism-based treatment approaches. *Brain Research Reviews* **67**:282-310.

Biggs JE, Stemkowski PL, Knaus E.E, Chowdhury MA, Ballanyi K and Smith P.A. (2015) Suppression of Network Activity in Dorsal Horn by Gabapentin Permeation of TRPV1 Channels; Implications for Drug Access to Cytoplasmic Targets. *Neurosci Lett* **584**:397-402.

Biggs JE, Boakye PA, Ganesan N, Stemkowski PL, Lantero A, Ballanyi K and Smith PA (2014) Analysis of the long-term actions of gabapentin and pregabalin in dorsal root ganglia and substantia gelatinosa. *J Neurophysiol* **112**:2398-2412.

Chen T, Koga K, Descalzi G, Qiu S, Wang J, Zhang LS, Zhang ZJ, He XB, Qin X, Xu FQ, Hu J, Wei F, Huganir RL, Li YQ and Zhuo M (2014a) Postsynaptic potentiation of corticospinal projecting neurons in the anterior cingulate cortex after nerve injury. *Mol Pain* **10**:33.

Chen T, OGÇÖDen G, Song Q, Koga K, Zhang MM and Zhuo M (2014b) Adenylyl cyclase subtype 1 is essential for late-phase long term potentiation and spatial propagation of synaptic responses in the anterior cingulate cortex of adult mice. *Mol Pain* **10**:65.

Coderre TJ, Kumar N, Lefebvre CD and Yu JS (2005) Evidence that gabapentin reduces neuropathic pain by inhibiting the spinal release of glutamate. *J Neurochem* **94**:1131-1139.

Costigan M, Scholz J and Woolf CJ (2009) Neuropathic pain: a maladaptive response of the nervous system to damage. *Annu Rev Neurosci* **32**:1-32.

Coull JA, Boudreau D, Bachand K, Prescott SA, Nault F, Sik A, De Koninck P and de Koninck Y (2003) Trans-synaptic shift in anion gradient in spinal lamina I neurons as a mechanism of neuropathic pain. *Nature* **424**:938-942.

Decosterd I and Woolf CJ (2000) Spared nerve injury: an animal model of persistent peripheral neuropathic pain. *Pain* **87**:149-158.

Dolphin AC (2012) Calcium channel auxiliary alpha2delta and beta subunits: trafficking and one step beyond. *Nat Rev Neurosci* **13**:542-555.

Dolphin AC (2013) The alpha2delta subunits of voltage-gated calcium channels. *Biochim Biophys Acta* **1828**:1541-1549.

Dolphin AC (2016) Voltage-gated calcium channels and their auxiliary subunits: physiology and pathophysiology and pharmacology. *J Physiol* **594**:5369-5390.

Eto K, Wake H, Watanabe M, Ishibashi H, Noda M, Yanagawa Y and Nabekura J (2011) Inter-regional contribution of enhanced activity of the primary somatosensory cortex to the anterior cingulate cortex accelerates chronic pain behavior. *J Neurosci* **31**:7631-7636.

Field MJ, Oles RJ, Lewis AS, McCleary S, Hughes J and Singh L (1997) Gabapentin (neurontin) and S-(+)-3-isobutylgaba represent a novel class of selective antihyperalgesic agents. *Br J Pharmacol* **121**:1513-1522.

Field MJ, Cox PJ, Stott E, Melrose H, Offord J, Su TZ, Bramwell S, Corradini L, England S, Winks J, Kinloch RA, Hendrich J, Dolphin AC, Webb T and Williams D (2006) Identification of the {alpha}2-{delta}-1 subunit of voltage-dependent calcium channels as a molecular target for pain mediating the analgesic actions of pregabalin. *PNAS* **103**:17537-17542.

Finnerup NB, Attal N, Haroutounian S, McNicol E, Baron R, Dworkin RH, Gilron I, Haanpaa M, Hansson P, Jensen TS, Kamerman PR, Lund K, Moore A, Raja SN, Rice AS, Rowbotham M, Sena E, Siddall P, Smith BH and Wallace M (2015) Pharmacotherapy for neuropathic pain in adults: a systematic review and meta-analysis. *Lancet Neurol* **14**:162-173.

Gee NS, Brown JP, Dissanayake VU, Offord J, Thurlow R and Woodruff GN (1996) The novel anticonvulsant drug, gabapentin (Neurontin), binds to the alpha2delta subunit of a calcium channel. *J Biol Chem* **271**:5768-5776.

Grudt TJ and Perl ER (2002) Correlations between neuronal morphology and electrophysiological features in the rodent superficial dorsal horn. *J Physiol* **540**:189-207.

Harte SE, Meyers JB, Donahue RR, Taylor BK and Morrow TJ (2016) Mechanical Conflict System: A Novel Operant Method for the Assessment of Nociceptive Behavior. *PLoS One* **11**:e0150164.

Hendrich J, Bauer CS and Dolphin AC (2012) Chronic pregabalin inhibits synaptic transmission between rat dorsal root ganglion and dorsal horn neurons in culture. *Channels (Austin)* **6**:124-132.

Hendrich J, Van Minh AT, Heblich F, Nieto-Rostro M, Watschinger K, Striessnig J, Wratten J, Davies A and Dolphin AC (2008) Pharmacological disruption of calcium channel trafficking by the {alpha}2{delta} ligand gabapentin. *Proc Natl Acad Sci U S A* **105**:3628-3633.

Hoppa MB, Lana B, Margas W, Dolphin AC and Ryan TA (2012) alpha2delta expression sets presynaptic calcium channel abundance and release probability. *Nature* **486**:122-125.

Hunter JC, Gogas KR, Hedley LR, Jacobson LO, Kassotakis L, Thompson J and Fontana DJ (1997) The effect of novel anti-epileptic drugs in rat experimental models of acute and chronic pain. *Eur J Pharmacol* **324**:153-160.

Kadurin I, Ferron L, Rothwell SW, Meyer JO, Douglas LR, Bauer CS, Lana B, Margas W, Alexopoulos O, Nieto-Rostro M, Pratt WS and Dolphin AC (2016) Proteolytic maturation of alpha2delta represents a checkpoint for activation and neuronal trafficking of latent calcium channels. *Elife* **5**.

Kayser V and Christensen D (2000) Antinociceptive effect of systemic gabapentin in mononeuropathic rats, depends on stimulus characteristics and level of test integration. *Pain* **88**:53-60.

Kim KJ, Yoon YW and Chung JM (1997) Comparison of three rodent models of neuropathic pain. *Exp Brain Res* **113**:200-206.

Kim SK, Eto K and Nabekura J (2012) Synaptic structure and function in the mouse somatosensory cortex during chronic pain: in vivo two-photon imaging. *Neural Plast* **2012**:640259.

Komagata S, Tamaki K, Hishida R, Takeshita N and Shibuki K (2011) Nociceptive cortical responses during capsaicin-induced tactile allodynia in mice with spinal dorsal column lesioning. *Neurosci Res* **69**:348-351.

Kumar N, Cherkas PS, Varathan V, Miyamoto M, Chiang CY, Dostrovsky JO, Sessle BJ and Coderre TJ (2013) Systemic pregabalin attenuates facial hypersensitivity and noxious stimulus-evoked release of glutamate in medullary dorsal horn in a rodent model of trigeminal neuropathic pain. *Neurochem Int* **62**:831-835.

Labrakakis C, Lorenzo LE, Bories C, Ribeiro-da-Silva A and De Koninck Y (2009) Inhibitory coupling between inhibitory interneurons in the spinal cord dorsal horn. *Molecular Pain* **5**:24.

Lana B, Page KM, Kadurin I, Ho S, Nieto-Rostro M and Dolphin AC (2016) Thrombospondin-4 reduces binding affinity of [(3)H]-gabapentin to calcium-channel alpha2delta-1-subunit but does not interact with alpha2delta-1 on the cell-surface when co-expressed. *Sci Rep* **6**:24531.

Larsen MS, Keizer R, Munro G, Mork A, Holm R, Savic R and Kreilgaard M (2016) Pharmacokinetic/Pharmacodynamic Relationship of Gabapentin in a CFA-induced Inflammatory Hyperalgesia Rat Model. *Pharm Res*.

Legrain V, Iannetti GD, Plaghki L and Mouraux A (2011) The pain matrix reloaded: a salience detection system for the body. *Prog Neurobiol* **93**:111-124.

Li CY, Zhang XL, Matthews EA, Li KW, Kurwa A, Boroujerdi A, Gross J, Gold MS, Dickenson AH, Feng G and Luo ZD (2006) Calcium channel alpha2delta1 subunit mediates spinal hyperexcitability in pain modulation. *Pain* **125**:20-34.

Li CY, Song YH, Higuera ES and Luo ZD (2004) Spinal Dorsal Horn Calcium Channel {alpha}2{delta}-1 Subunit Upregulation Contributes to Peripheral Nerve Injury-Induced Tactile Allodynia. *Journal of Neuroscience* **24**:8494-8499.

Lu Y and Perl ER (2005) Modular Organization of Excitatory Circuits between Neurons of the Spinal Superficial Dorsal Horn (Laminae I and II). *Journal of Neuroscience* **25**:3900-3907.

Luo ZD, Calcutt NA, Higuera ES, Valder CR, Song YH, Svensson CI and Myers RR (2002) Injury type-specific calcium channel alpha 2 delta-1 subunit up-regulation in rat neuropathic pain models correlates with antiallodynic effects of gabapentin. *J Pharmacol Exp Ther* **303**:1199-1205.

Luo ZD, Chaplan SR, Higuera ES, Sorkin LS, Stauderman KA, Williams ME and Yaksh TL (2001) Upregulation of Dorsal Root Ganglion {alpha}2{delta} Calcium Channel Subunit and Its Correlation with Allodynia in Spinal Nerve-Injured Rats. *Journal of Neuroscience* **21**:1868-1875.

Mogil JS (2009) Animal models of pain: progress and challenges. *Nat Rev Neurosci* **10**:283-294.

Moore KA, Baba H and Woolf CJ (2002) Gabapentin -- Actions on adult superficial dorsal horn neurons. *Neuropharmacology* **43**:1077-1081.

Moore RA, Wiffen PJ, Derry S, Toelle T and Rice AS (2014) Gabapentin for chronic neuropathic pain and fibromyalgia in adults. *Cochrane Database Syst Rev* **4**:CD007938.

Mosconi T and Kruger L (1996) Fixed-diameter polyethylene cuffs applied to the rat sciatic nerve induce a painful neuropathy: ultrastructural morphometric analysis of axonal alterations. *Pain* **64**:37-57.

Pan B, Guo Y, Wu HE, Park J, Trinh VN, Luo ZD and Hogan QH (2016) Thrombospondin-4 divergently regulates voltage-gated Ca2+ channel subtypes in sensory neurons after nerve injury. *Pain*.

Pan HL, Eisenach JC and Chen SR (1999) Gabapentin suppresses ectopic nerve discharges and reverses allodynia in neuropathic rats. *J Pharmacol Exp Ther* **288**:1026-1030.

Patel R and Dickenson AH (2016) Neuronal Hyperexcitability in the Ventral Posterior Thalamus of Neuropathic Rats: Modality Selective Effects of Pregabalin. *J Neurophysiol*jn.

Pertin M, Gosselin RD and Decosterd I (2012) The spared nerve injury model of neuropathic pain. *Methods Mol Biol* **851**:205-212.

Pitcher GM and Henry JL (2008) Governing role of primary afferent drive in increased excitation of spinal nociceptive neurons in a model of sciatic neuropathy. *Exp Neurol* **214**:219-228.

Potter LE, Paylor JW, Suh JS, Tenorio G, Caliaperumal J, Colbourne F, Baker G, Winship I and Kerr BJ (2016) Altered excitatory-inhibitory balance within somatosensory cortex is associated with enhanced plasticity and pain sensitivity in a mouse model of multiple sclerosis. *J Neuroinflammation* **13**:142.

Punnakkal P, von SC, Haenraets K, Wildner H and Zeilhofer HU (2014) Morphological, Biophysical and Synaptic Properties of Glutamatergic Neurons of the Mouse Spinal Dorsal Horn. *J Physiol* **592**:759-776.

Sandkuhler J (2009) Models and mechanisms of hyperalgesia and allodynia. *Physiol Rev* **89**:707-758.

Sharma U, Griesing T, Emir B and Young JP, Jr. (2010) Time to onset of neuropathic pain reduction: A retrospective analysis of data from nine controlled trials of pregabalin for painful diabetic peripheral neuropathy and postherpetic neuralgia. *Am J Ther* **17**:577-585.

Stebbing MJ, Balasubramanyan S and Smith PA (2016) Calbindin-D-28K like immunoreactivity in superficial dorsal horn neurons and effects of sciatic chronic constriction injury. *Neuroscience* **324**:330-343.

Stemkowski PL and Smith PA (2012) Long-term IL-1beta exposure causes subpopulation-dependent alterations in rat dorsal root ganglion neuron excitability. *J Neurophysiol* **107**:1586-1597.

Todd AJ (2010) Neuronal circuitry for pain processing in the dorsal horn. *Nat Rev Neurosci* **11**:823-836.

Todd AJ and Spike RC (1993) The localization of classical transmitters and neuropeptides within neurons in laminae I-III of the mammalian spinal dorsal horn. *Prog Neurobiol* **41**:609-645.

Torrance N, Smith BH, Bennett MI and Lee AJ (2006) The epidemiology of chronic pain of predominantly neuropathic origin. Results from a general population survey. *J Pain* **7**:281-289.

Treede R-D, Jensen TS, Campbell JN, Cruccu G, Dostrovsky JO, Griffin JW, Hansson P, Hughes R, Nurmikko T and Serra J (2008) Neuropathic pain: Redefinition and a grading system for clinical and research purposes. *Neurology* **70**:1630-1635.

Winship IR and Murphy TH (2008) In vivo calcium imaging reveals functional rewiring of single somatosensory neurons after stroke. *J Neurosci* **28**:6592-6606.

Winship IR, Plaa N and Murphy TH (2007) Rapid astrocyte calcium signals correlate with neuronal activity and onset of the hemodynamic response in vivo. *J Neurosci* **27**:6268-6272.

Yasaka T, Tiong SY, Hughes DI, Riddell JS and Todd AJ (2010) Populations of inhibitory and excitatory interneurons in lamina II of the adult rat spinal dorsal horn revealed by a combined electrophysiological and anatomical approach. *Pain* **151**:475-488.

Zamponi GW, Striessnig J, Koschak A and Dolphin AC (2015) The Physiology, Pathology, and Pharmacology of Voltage-Gated Calcium Channels and Their Future Therapeutic Potential. *Pharmacol Rev* **67**:821-870.

Zhou C and Luo ZD (2015) Nerve injury-induced calcium channel alpha-2-delta-1 protein dysregulation leads to increased pre-synaptic excitatory input into deep dorsal horn neurons and neuropathic allodynia. *European Journal of Pain*Feb 17. doi: 10.1002/ejp.656. [Epub ahead of print].

Zhuo M (2008) Cortical excitation and chronic pain. *Trends Neurosci* **31**:199-207.

ACKNOWLEDGEMENTS

We thank Gail Rauw, Nataliya Bukhanova, Twinkle Joy and Bin Dong for technical assistance.

Supported by the Natural Sciences and Engineering Research Council (NSERC, Ottawa, ON Canada) and by the Canadian Foundation for Innovation (CFI) awards to PAS and KB

AUTHORSHIP CONTRIBUTIONS

Participated in research design: Alles, Bandet, Winship, Baker, Ballanyi, Smith

Conducted Experiments: Alles, Bandet, Noh, Eppler

Performed Data Analysis: Alles, Bandet Eppler

Wrote or contributed to the writing of the manuscript: Alles, Smith, Eppler

Developed Methodologies and Provided Additional Laboratory Facilities: Ballanyi, Noh, Baker, Winship

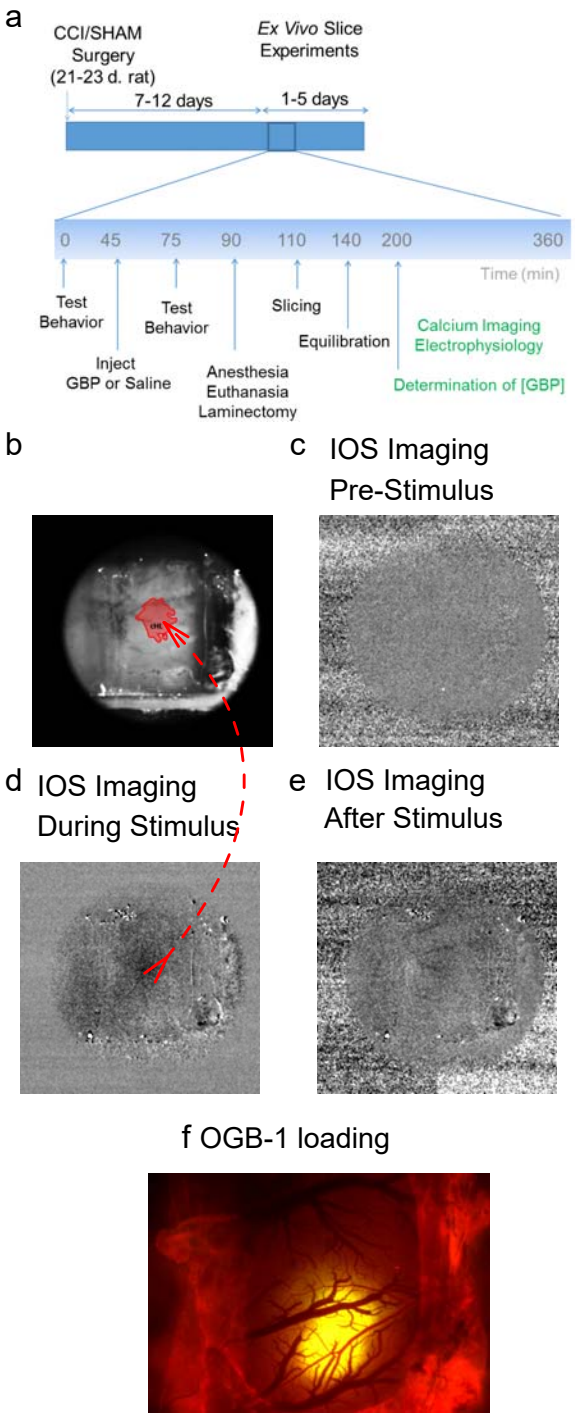
a
CCI/SHAM Surgery (21-23 d. rat)
Ex Vivo Slice Experiments
7-12 days
1-5 days
0 45 75 90 110 140 200 360
Time (min)
Test Behavior
Test Behavior
Slicing
Equilibration
Calcium Imaging Electrophysiology
Inject GBP or Saline
Anesthesia Euthanasia Laminectomy
Determination of [GBP]
b
c IOS Imaging Pre-Stimulus
d IOS Imaging During Stimulus
e IOS Imaging After Stimulus
f OGB-1 loading

Figure 1

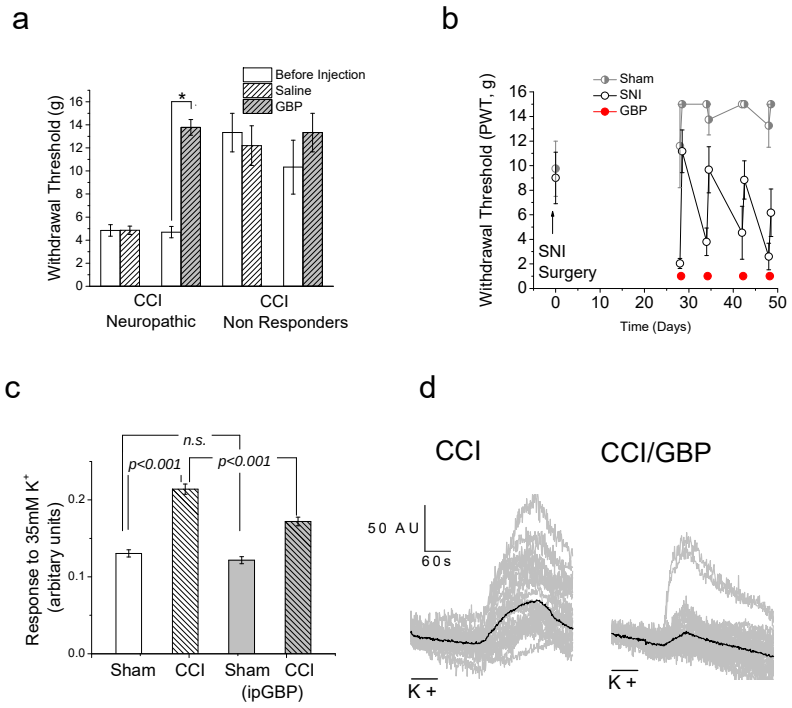
a
b
c
d
Before Injection
Saline
GBP
Withdrawal Threshold (g)
CCI
Neuropathic
CCI
Non Responders
Sham
SNI
GBP
Withdrawal Threshold (PWT, g)
SNI
Surgery
Time (Days)
n.s.
p<0.001
p<0.001
Response to 35mM K+
(arbitary units)
Sham
CCI
Sham
(ipGBP)
CCI
CCI/GBP
50 AU
60s
K +
K +

Figure 2

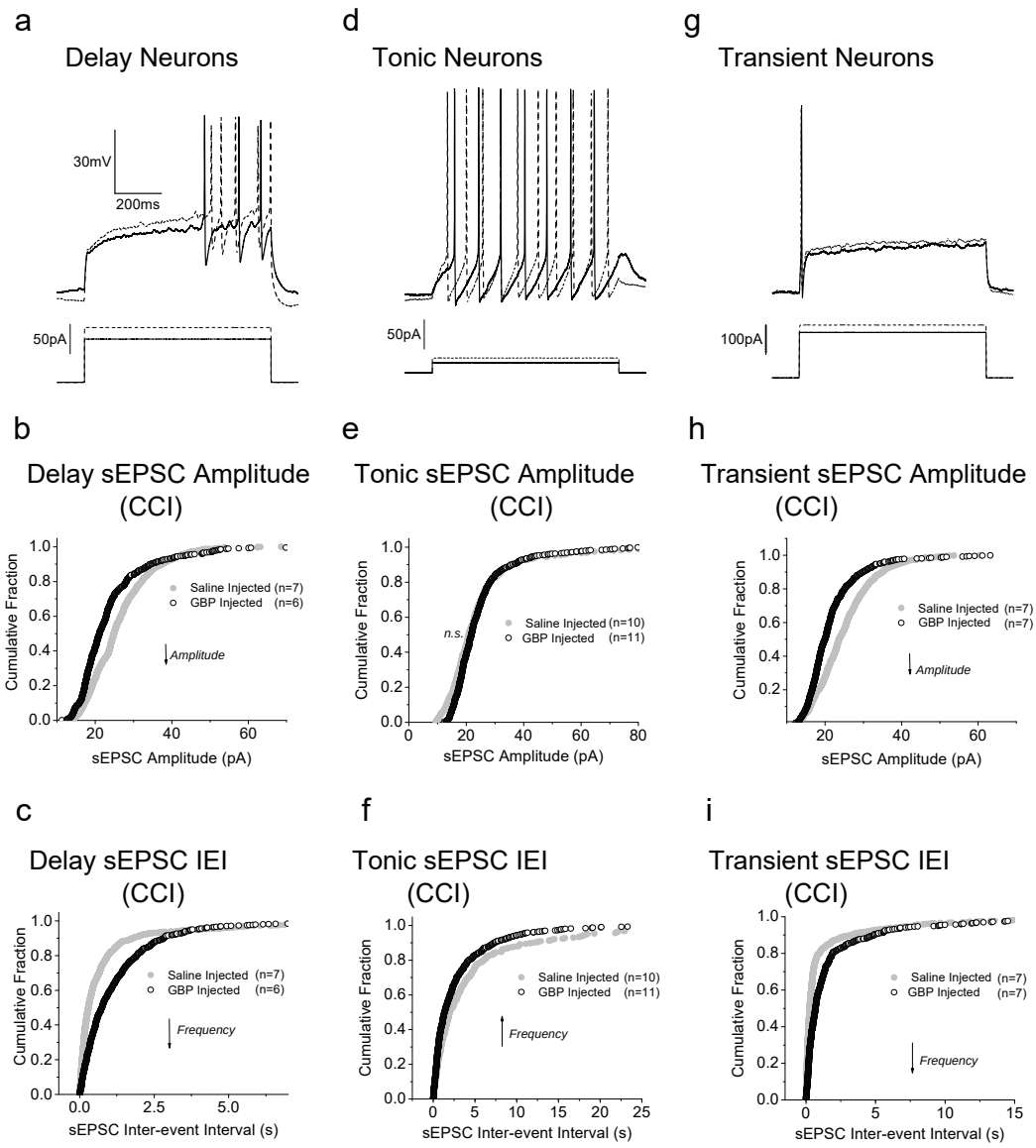
a
Delay Neurons
30mV
200ms
50pA
d
Tonic Neurons
50pA
g
Transient Neurons
100pA
b
Delay sEPSC Amplitude (CCI)
Cumulative Fraction
Saline Injected (n=7)
GBP Injected (n=6)
Amplitude
sEPSC Amplitude (pA)
e
Tonic sEPSC Amplitude (CCI)
n.s.
Saline Injected (n=10)
GBP Injected (n=11)
sEPSC Amplitude (pA)
h
Transient sEPSC Amplitude (CCI)
Saline Injected (n=7)
GBP Injected (n=7)
Amplitude
sEPSC Amplitude (pA)
c
Delay sEPSC IEI (CCI)
Saline Injected (n=7)
GBP Injected (n=6)
Frequency
sEPSC Inter-event Interval (s)
f
Tonic sEPSC IEI (CCI)
Saline Injected (n=10)
GBP Injected (n=11)
Frequency
sEPSC Inter-event Interval (s)
i
Transient sEPSC IEI (CCI)
Saline Injected (n=7)
GBP Injected (n=7)
Frequency
sEPSC Inter-event Interval (s)

Figure 3

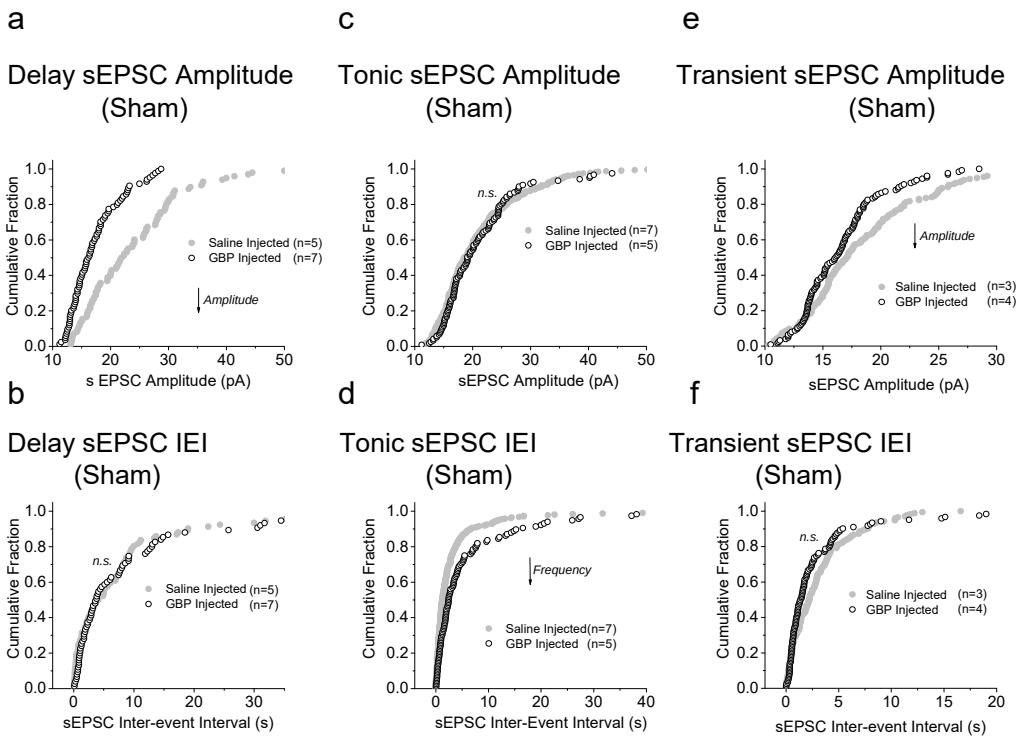
a
Delay sEPSC Amplitude
(Sham)
Cumulative Fraction
s EPSC Amplitude (pA)
Saline Injected (n=5)
GBP Injected (n=7)
Amplitude
c
Tonic sEPSC Amplitude
(Sham)
n.s.
sEPSC Amplitude (pA)
Saline Injected (n=7)
GBP Injected (n=5)
e
Transient sEPSC Amplitude
(Sham)
Amplitude
sEPSC Amplitude (pA)
Saline Injected (n=3)
GBP Injected (n=4)
b
Delay sEPSC IEI
(Sham)
n.s.
sEPSC Inter-event Interval (s)
Saline Injected (n=5)
GBP Injected (n=7)
d
Tonic sEPSC IEI
(Sham)
Frequency
sEPSC Inter-Event Interval (s)
Saline Injected(n=7)
GBP Injected (n=5)
f
Transient sEPSC IEI
(Sham)
n.s.
sEPSC Inter-event Interval (s)
Saline Injected (n=3)
GBP Injected (n=4)

Figure 4

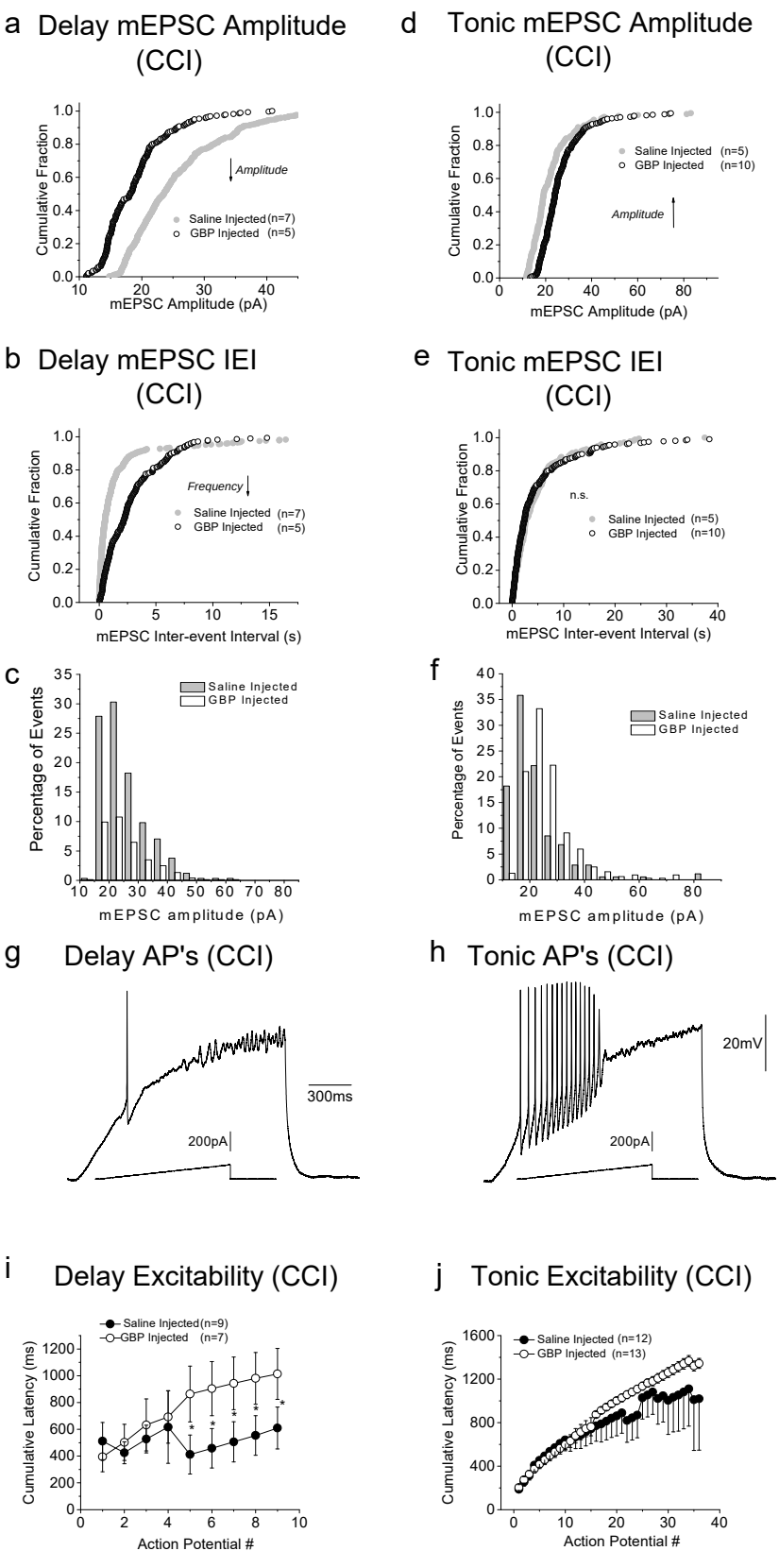
a Delay mEPSC Amplitude (CCI)
Cumulative Fraction
mEPSC Amplitude (pA)
Amplitude
Saline Injected (n=7)
GBP Injected (n=5)
d Tonic mEPSC Amplitude (CCI)
Cumulative Fraction
mEPSC Amplitude (pA)
Saline Injected (n=5)
GBP Injected (n=10)
Amplitude
b Delay mEPSC IEI (CCI)
Cumulative Fraction
mEPSC Inter-event Interval (s)
Frequency
Saline Injected (n=7)
GBP Injected (n=5)
e Tonic mEPSC IEI (CCI)
Cumulative Fraction
mEPSC Inter-event Interval (s)
n.s.
Saline Injected (n=5)
GBP Injected (n=10)
c
Percentage of Events
mEPSC amplitude (pA)
Saline Injected
GBP Injected
f
Percentage of Events
mEPSC amplitude (pA)
Saline Injected
GBP Injected
g Delay AP's (CCI)
300ms
200pA
h Tonic AP's (CCI)
20mV
200pA
i Delay Excitability (CCI)
Cumulative Latency (ms)
Action Potential #
Saline Injected (n=9)
GBP Injected (n=7)
j Tonic Excitability (CCI)
Cumulative Latency (ms)
Action Potential #
Saline Injected (n=12)
GBP Injected (n=13)

Figure 5

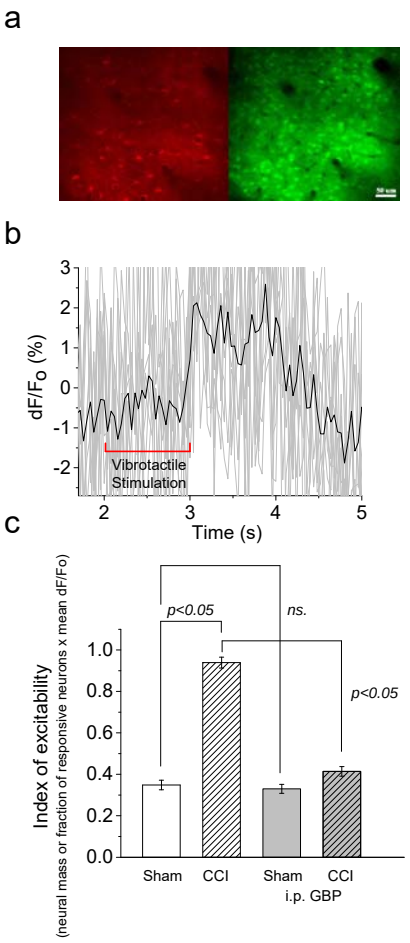
a
b
dF/F0 (%)
Vibrotactile
Stimulation
Time (s)
c
Index of excitability
(neural mass or fraction of responsive neurons x mean dF/Fo)
p<0.05
ns.
p<0.05
Sham
CCI
Sham
CCI
i.p. GBP

Figure 6